M044

Gabor Domain Analysis of Q in the Near-surface

R.J. Ferguson* (University of Calgary), G.F. Margrave (University of Calgary) & K.W. Hall (University of Calgary)

SUMMARY

We present a Q estimation method where analysis is done in the Gabor domain.
There, attenuation is estimated as a function of frequency (f), and Q (f) is computed through inversion of attenuation.

We provide an example based on a 7-level, near-offset VSP consisting of 3-component receivers and sweeps.
Eight, narrowband sweeps are used to span 10 Hz - 250 Hz for each source orientation.

Two subunits are identified within the local formation that correspond to an expected 50 m of unsaturated media underlain by an aquifer. Our results demonstrate that attenuation varies near-linearly with frequency for the 95 m depth range. Strong values of attenuation that increase with frequency are found in the unsaturated unit, and weaker, decreasing attenuation is found in the saturated unit.

Introduction

We present a Q estimation method based on traveltime derivatives applied to multilevel vertical seismic profile (VSP) acquisition. Long, narrowband vibroseis sweeps provide approximately monochromatic wavefields over short time windows, and analysis is done in the Gabor domain. There, attenuation β is estimated as a function of frequency f, and $Q\,(f)$ is computed through inversion of β.

We provide an example based on a 7-level, near-offset VSP. Each VSP level consists of a 3-component receiver with inline, crossline, and vertical sweeps. Eight, narrowband sweeps are used to span 10 Hz - 250 Hz for each source orientation, and they are found to help reduce noise in the data due to baseplate harmonics.

Two subunits are identified within the local formation that correspond to an expected 50 m of unsaturated media underlain by an aquifer. Our results demonstrate that β varies near-linearly with frequency for the 95 m depth range, Strong values of β that increase with f are found in the unsaturated unit, and weaker, decreasing β is found in the saturated unit.

Q for the formation is estimated only approximately due to excessive powerline noise and and strong harmonics in the well. For both units and the overall formation, Q increases linearly with f until about 100 Hz.

Theory

Propagation of planewave G in a homogeneous attenuative medium is modelled by

$$G\,(\tau, f) = A\,(f)\; e^{-\beta(f)\,\tau}\, e^{i\,\phi(\tau,f)}, \tag{1}$$

where f is frequency in Hz, A is source amplitude, ϕ is phase, τ is traveltime between source and receiver, and attenuation β is given by

$$\beta\,(f) = \pi\, f/Q. \tag{2}$$

Quality factor Q is characteristic of the effective attenuation of the medium between source and receiver (Jannsen et al., 1985). Equation 1 forms the basis for many Q estimation processes most notably the spectral ratio method (Båth, 1974). Phase ϕ describes the kinematics and dispersion of wave propagation and is of interest in seismic velocity inversion (Sun et al., 2009; Toverud and Ursin, 2005). Power $G\,G^{\dagger}$ of equation 1 eliminates the phase term according to

$$G\,(\tau, f)\; G\,(\tau, f)^{\dagger} = A^2\,(f)\; e^{-2\,\beta(f)\,\tau}, \tag{3}$$

and it returns a real valued, positive result. So, for $A > 0$,

$$\log\left\{\sqrt{G\,(\tau, f)\; G^{\dagger}\,(\tau, f)}\right\} = \log\left\{A\,(f)\right\} - \beta\,(f)\;\tau, \tag{4}$$

is a linear function with slope β. For a multidepth VSP, τ is traveltime from receiver level to receiver level, and $\beta\,(f)$ is obtained if we differentiate equation 4 along τ. Equations 2 and 4 suggest that if $\log\sqrt{G\,G^{\dagger}}$ by least-squares fit of equation 4 in τ we may estimate Q for all f. We assume here that Q is τ independent and we use formation by formation analysis to obtain $Q\,(\tau)$.

Data acquisition

To explore Q prediction based on equation 4, we acquired a 10 m offset VSP with a multilevel (7 levels spanning 10-95 m), 3-component downhole tool, a number of narrow frequency-band sweeps with sources in the vertical (V), inline horizontal (H_1), and crossline horizontal (H_2) directions. A summary of the sweeps is found in the legend on Figure 1.

Data processing

During VSP acquisition, vertical-component surface recordings were made for all sweeps, and these data are used to normalize all VSPs. Each uncorrelated VSP component is corrected for spherical spreading (Newman, 1973), filtered to within it's sweep range, and Gabor transformed (Sun et al., 2009). Power spectrum $G\,G^{\dagger}$ for the vector wavefield is is then computed as a sum of the spectra over the 3 components. For each depth, power spectra for all sweeps are summed as in Figure 1 for sources V (a) and H_2 (b) (H_1 not shown). Columns in these Gabor matrices quantify the power of one frequency f spread over sweeptime t (distinct from traveltime τ). Because $\beta\,(f)$ (equation 4) is the result of a scaled τ derivative, overlapping sweeps may be summed along sweep time (vertical axes Figure 1) as long as sweep overlap is consistent depth-to-depth.

Annotated lines on Figure 1 indicate expected sweep ranges. All sweeps are present for V. A strong event at $\sim$ 40 Hz is apparent on V and to a lesser extent on H_1 (not shown) and on H_2, and a baseplate harmonic is apparent on V between 35 and 40 Hz and 0 and 5 s. It also excites amplitudes at 40 Hz. The 40 Hz event is absent on the surface data and is attributed to some property of the well.

Problems associated with H_1 and H_2 result in a number of bad or missing sweeps (Figure 1b indicates sweep 145-250 Hz is missing). Where this occurs, a reference 14-250 Hz sweep is filtered appropriately and scaled (Figure 1b between 10 and 20 s). This replacement does allow leakage of baseplate harmonics that originate in the lower part of the broadband sweep as seen between 0 and 8 seconds. The broadband sweep is otherwise excluded from analysis.

Q estimation

For each depth and each source, Gabor spectra are integrated along sweep time, then square root and natural logarithm are applied according to equation 4. Frequency curves are plotted as surfaces in Figure 2. Red dots along τ indicate traveltimes to each receiver. A strong amplitude associated with $\sim$ 40 Hz is apparent on Figure 2a (V). Lesser peaks are associated with 60 Hz, 120 Hz, and 180 Hz. The 40 Hz amplitude is less apparent on the H_2 source data (Figure 2b), and the 60 Hz related peaks are very strong. $\log A$ changes abruptly for V, H_1 (not shown), and H_2 at $\approx$ 0.26 s (≈ 50 m) for all f and coincides with the expected boundary between an upper unit (unsaturated) and a lower unit (groundwater saturated).

Data from Figure 2 are differentiated along τ (traveltime), and β (RMS) is computed for each f. The resulting $\beta\,(f)$ are plotted in Figure 3 for each source. Figure 3a indicates effective β for the formation increases with f. Strong noise is present at $\approx$ 40 Hz, and at 60, 120, and 180 Hz (powerline noise). For the upper unit (10-50 m, Figure 3b), β increases strongly with f, and noise is apparent at $\approx$ 40 Hz. Powerline noise is not significant. β is weaker and decreases with f in the lower unit (50-95 m, Figure 3c). The 40 Hz noise is absent, though powerline noise is is very strong.

Linear best-fits (Figure 3, dashed lines) are computed for each $\beta\,(f)$ (formation, unit 1, unit 2) and inverted for Q according to equation 2. Curves for Q_F (formation), $Q1$ (unit 1), and $Q2$ (unit 2) are plotted against f in Figure 4, and effective Q_e for the formation is computed according to

$$1/Q_e = \left[\tau_1/Q_1 + \tau_2/Q_2\right]/\tau, \tag{5}$$

where τ_1, and τ_2 are traveltimes in units 1 and 2, and $\tau = \tau_1 + \tau_2$ (Båth, 1974; Dasgupta and Clark, 1998). Q estimates all increase with f until about 100 Hz and then rise exponentially (not shown) and indicate, perhaps, the usable f range. Calculated Q_e (Figure 4, dashed line) does not lie close to Q_F (Figure 4, red line).

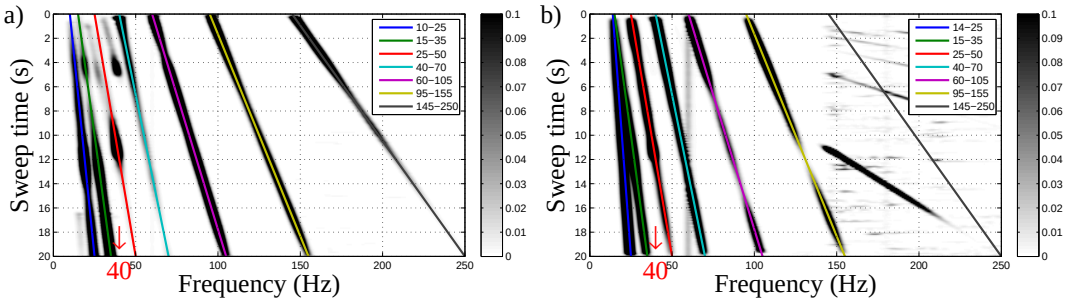

Figure 1 *Superimposed Gabor power spectra for $z = 50$ m. a) Source V. b) Source H_2.*

Discussion and Conclusions

In our traveltime-derivative approach to Q estimation applied to a real VSP, the Gabor domain is found to be useful as observed by others (Reine et al., 2009, for example). We use the Gabor domain to identify noise sources and verify sweep fidelity, and most importantly, we use it to estimate Q based on traveltimes of monochromatic wavefields in the subsurface. Our use of long, narrowband sweeps, reduces noise effects due to baseplate harmonics.

We identify a possible indicator for the transition from unsaturated to water saturated on our plots of $\log A\,(\tau, f)$ at ≈ 50 m[1]. From the $\log A$ data, we deduce attenuation β curves for the formation, and curves for the saturated (weak β, decreases with f) and unsaturated (strong β, increases with f) units. Due to significant noise still present in the data, and because of the small number of depths sampled, Q for the formation and units is estimated with β best-fits. Q values for the formation and both units increase with f below 100 Hz beyond which they rise exponentially. Measured Q for the formation and effective Q (calculated) are not in close agreement, so doubt is cast on all of the Q estimates. We anticipate that a 10-fold increase in the number of depth levels acquired, and greater attention to noise reduction in the field will improve Q estimates.

Acknowledgements

The authors thank Dr. Doug Schmitt of the University of Alberta and Dr. Peter Manning of CREWES for their assistance, and we thank NSERC of Canada and the sponsors of CREWES for their support of this work.

References

Båth, M. [1974] Spectral analysis in geophysics. In: Developments in solid earth geophysics. Elsevier Scientific Publishing Company, Amsterdam.

Dasgupta, R. and Clark, R.A. [1998] Estimation of Q from surface seismic reflection data. Geophysics, **63**(06), 2120–2128.

Jannsen, D., Voss, J. and Theilen, F. [1985] Comparison of methods to determine Q in shallow marine sediments from vertical reflection seismograms. Geophys. Prosp., **33**(04), 479–497.

Newman, P. [1973] Divergence effects in a layered earth. Geophysics, **38**(03), 481–488.

Reine, C., van der Baan, M. and Clark, R. [2009] The robustness of seismic attenuation measurements using fixed- and variable-window time-frequency transforms. Geophysics, **74**(2), WA123–WA135.

Sun, L.F., M., B. and Schmitt, D.R. [2009] Measuring velocity dispersion and attenuation in the exploration seismic frequency band. Geophysics, **74**(2), WA113–WA122, ISSN 2, doi:10.1190/1.3068426.

Toverud, T. and Ursin, B. [2005] Comparison of seismic attenuation models using zero-offset vertical seismic profiling (vsp) data. Geophysics, **70**(2), F17–F25, doi:10.1190/1.1884827.

[1] A watertable depth of 50 m is consistent with field observations.

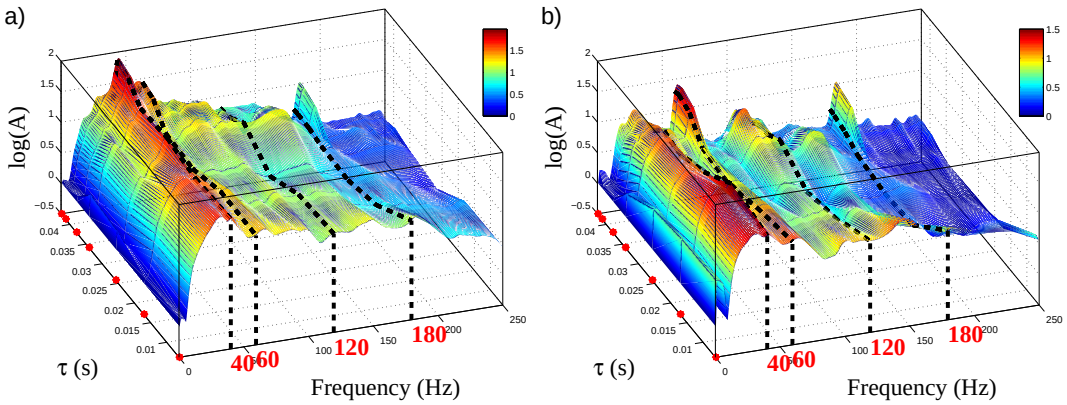

Figure 2 $\log A$, *where* $A = \sqrt{G\,G^{\dagger}}$ *(equation 4). a) Source* V*. b) Source* H_2*.*

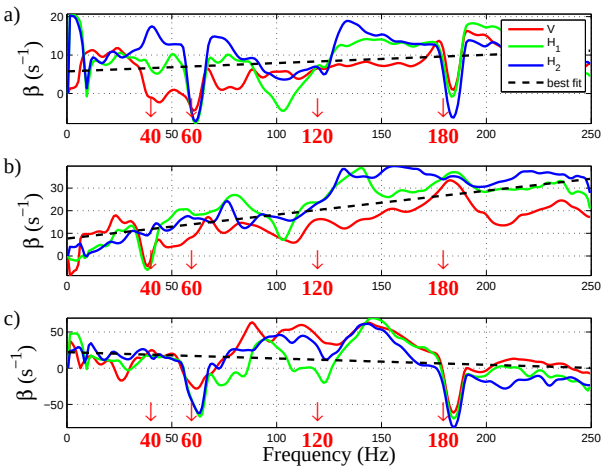

Figure 3 *Attenuation* β*. a) Depths 10-95 m. b) Depths 10-50 m. c) Depths 70-95 m.*

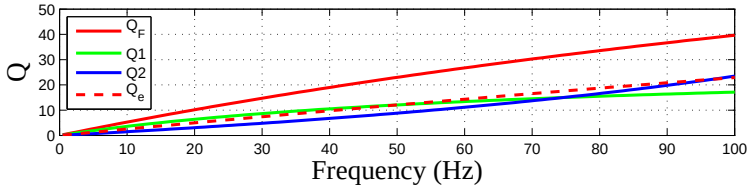

Figure 4 Q (f)*. a) Depths 10-95 m. b) Depths 10-50 m. c) Depths 50-95 m.*